Supporting Information for "Radar attenuation in Europa's ice shell: Obstacles and opportunities for constraining the shell thickness and its thermal structure"

Klára Kalousová[1,2], Dustin M. Schroeder[3], Krista M. Soderlund[4]

Contents of this file

1. Figures S1–S23
2. Tables S1–S2

Introduction This Supporting Information provides several supplementary figures. First, Figures S1–S13 depict temperature, heating rate (for the simulations where heating rate was considered), and two-way attenuation (computed while assuming low loss ice) as functions of horizontal coordinate x and depth for all the simulations from the main text (except the reference simulation for which these fields are depicted in Figures 1 and 3, respectively). Additionally, Figure S14 shows the two-way attenuation corresponding to temperature fields from Figure 1 computed while assuming high loss ice.

Second, we provide figures showing the results of simulations with temperature-dependent thermal conductivity (cf. Section 5.1 in the main text): Figures S15–S16 show temperature, heating rate (if it was considered), and two-way attenution for low loss ice; Figure S17 provides comparison of horizontally-averaged temperature profiles for simulations with constant and temperature-dependent thermal conductivity (and assuming the reference values of model parameters, i.e. η_0=10^{14} Pa s, E_a=5×10^4 J mol^{-1}, T_s=100 K, and two amplitudes of volumetric heating, H_m=0 and 5×10^{-6} W m^{-3}); and finally Figure S18 shows the two-way attenuation as a fuction of depth and shell thickness for the same simulations. Table S1 provides the values of maximal and minimal penetration depths for these simulations.

Third, we compare the results of the reference simulation with those computed while assuming different boundary conditions (periodic boundary condition on sides, simulation R1) or aspect ratios (λ=3 and λ=6, simulations R2 and R3, respectively, cf. also Section 5.5 in the main text): Figures S19–S21 show temperature and two-way attenution for low loss ice; Figure S22 provides comparison of horizontally-averaged temperature profiles for the reference simulation and simulations R1–R3; and finally Figure S23 shows the two-way attenuation as a fuction of depth and shell thickness for the same simulations. Table S2 provides the values of maximal and minimal penetration depths for these simulations.

[1]Jet Propulsion Laboratory, California Institute of Technology, 4800 Oak Grove Drive, Pasadena, CA 91109, USA.

[2]Charles University, Faculty of Mathematics and Physics, Department of Geophysics, V Holešovičkách 2, 180 00 Praha 8, Czech Republic.

[3]Stanford University, Department of Geophysics, School of Earth, Energy, and Environmental Sciences, 397 Panama Mall, Stanford, CA 94305, USA.

[4]The University of Texas at Austin, Institute for Geophysics, John A. & Katherine G. Jackson School of Geosciences, 10100 Burnet Rd., Austin, TX 78758-4445, USA.

0148-0227/17/$9.00

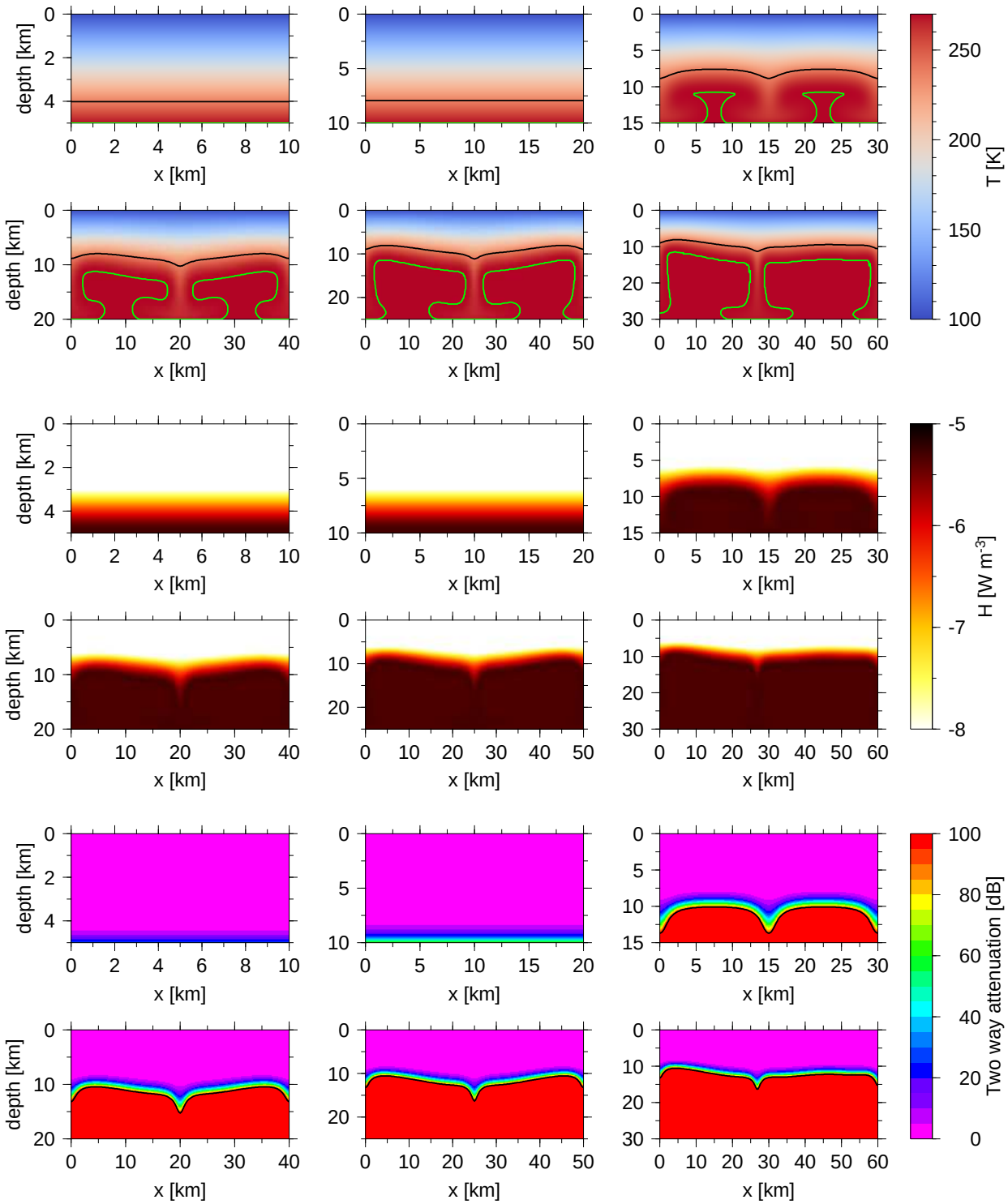

Figure S1: Results computed for: η_0=10^{14} Pa s, E_a=5×10^4 J mol^{-1}, T_s=100 K, H_m=5×10^{-6} W m^{-3}. Top: Temperature (black contour marks the eutectic temperature, T=237 K, green contour marks the melting temperature of 270 K), middle: heating rate, bottom: two-way attenuation for low loss ice (black contour marks the attenuation of 100 dB).

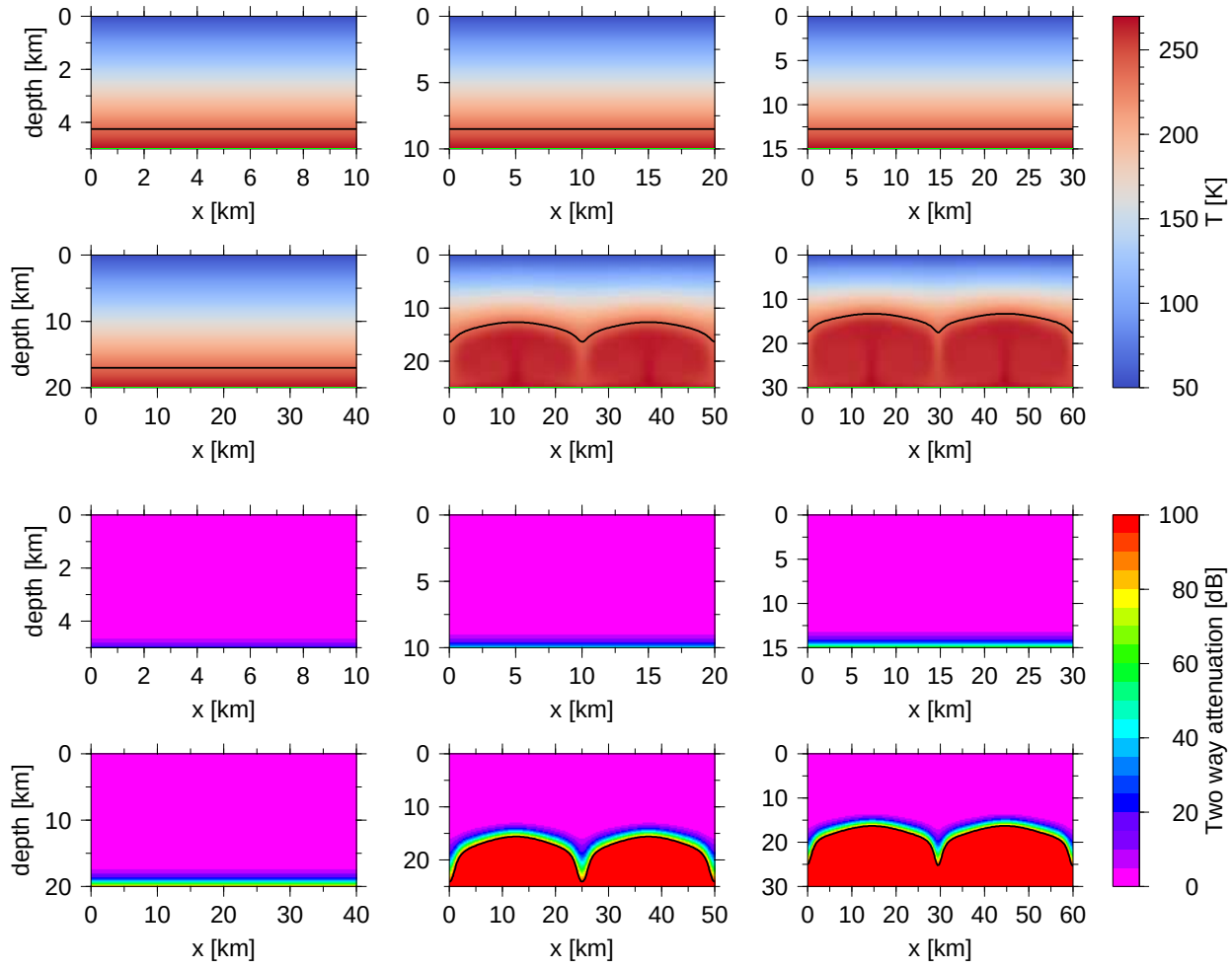

Figure S2: Results computed for: η_0=10^{14} Pa s, E_a=5×10^4 J mol^{-1}, T_s=50 K, H_m=0×10^{-6} W m^{-3}. Top: Temperature (black contour marks the eutectic temperature, T=237 K, green contour marks the melting temperature of 270 K), bottom: two-way attenuation for low loss ice (black contour marks the attenuation of 100 dB).

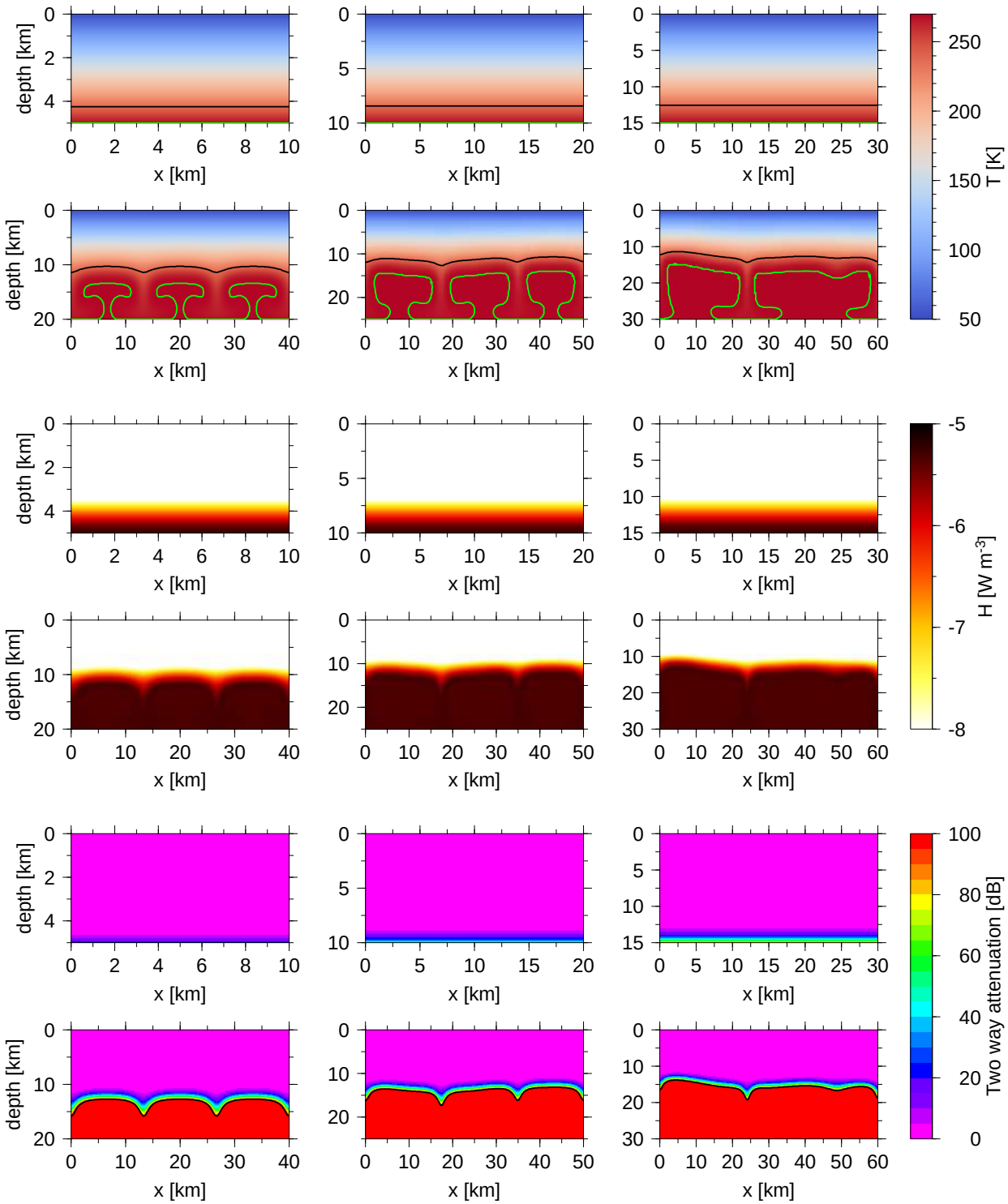

Figure S3: Results computed for: η_0=10^{14} Pa s, E_a=5×10^4 J mol^{-1}, T_s=50 K, H_m=5×10^{-6} W m^{-3}. Top: Temperature (black contour marks the eutectic temperature, T=237 K, green contour marks the melting temperature of 270 K), middle: heating rate, bottom: two-way attenuation for low loss ice (black contour marks the attenuation of 100 dB).

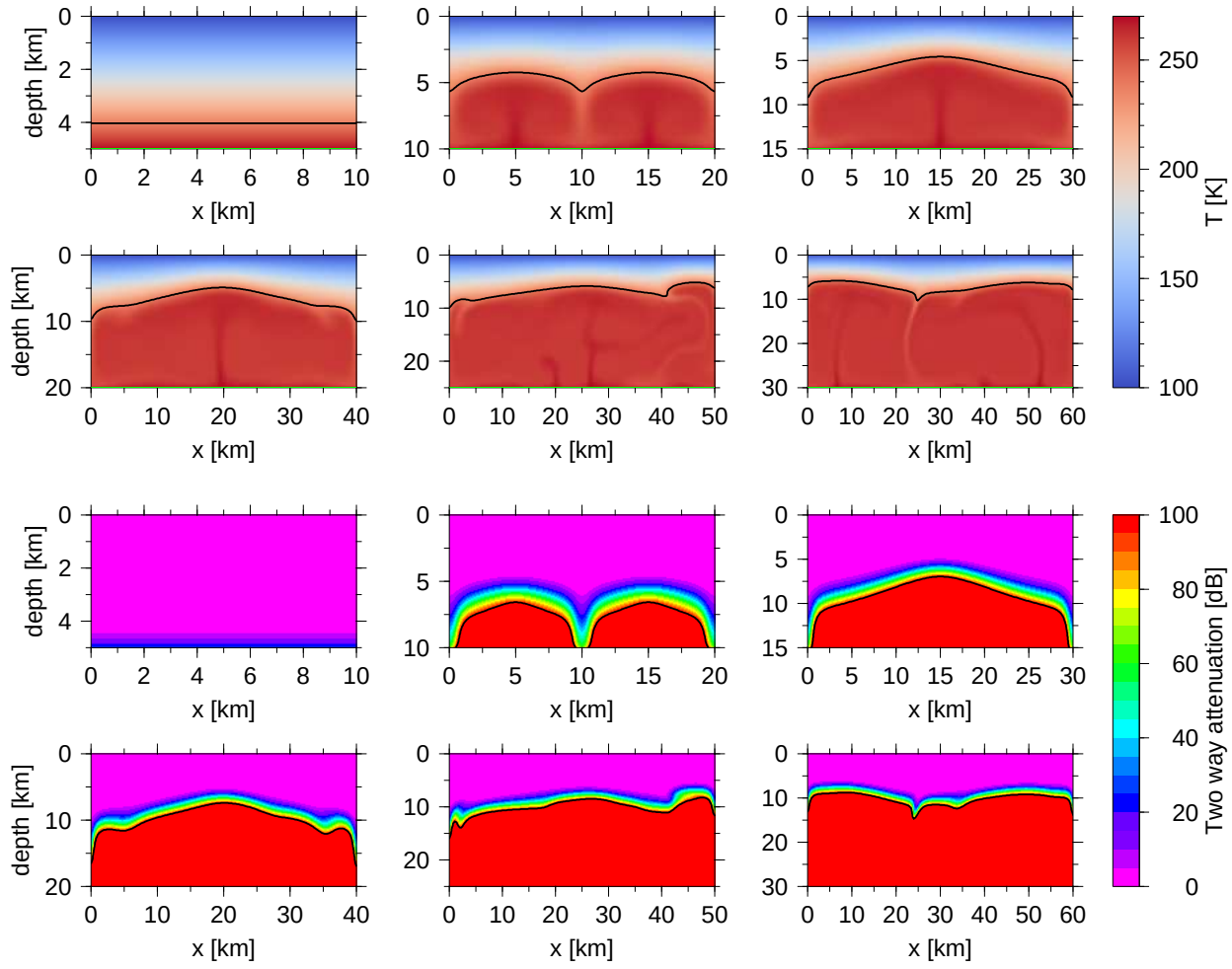

Figure S4: Results computed for: η_0=10^{13} Pa s, E_a=5×10^4 J mol^{-1}, T_s=100 K, H_m=0×10^{-6} W m^{-3}. Top: Temperature (black contour marks the eutectic temperature, T=237 K, green contour marks the melting temperature of 270 K), bottom: two-way attenuation for low loss ice (black contour marks the attenuation of 100 dB).

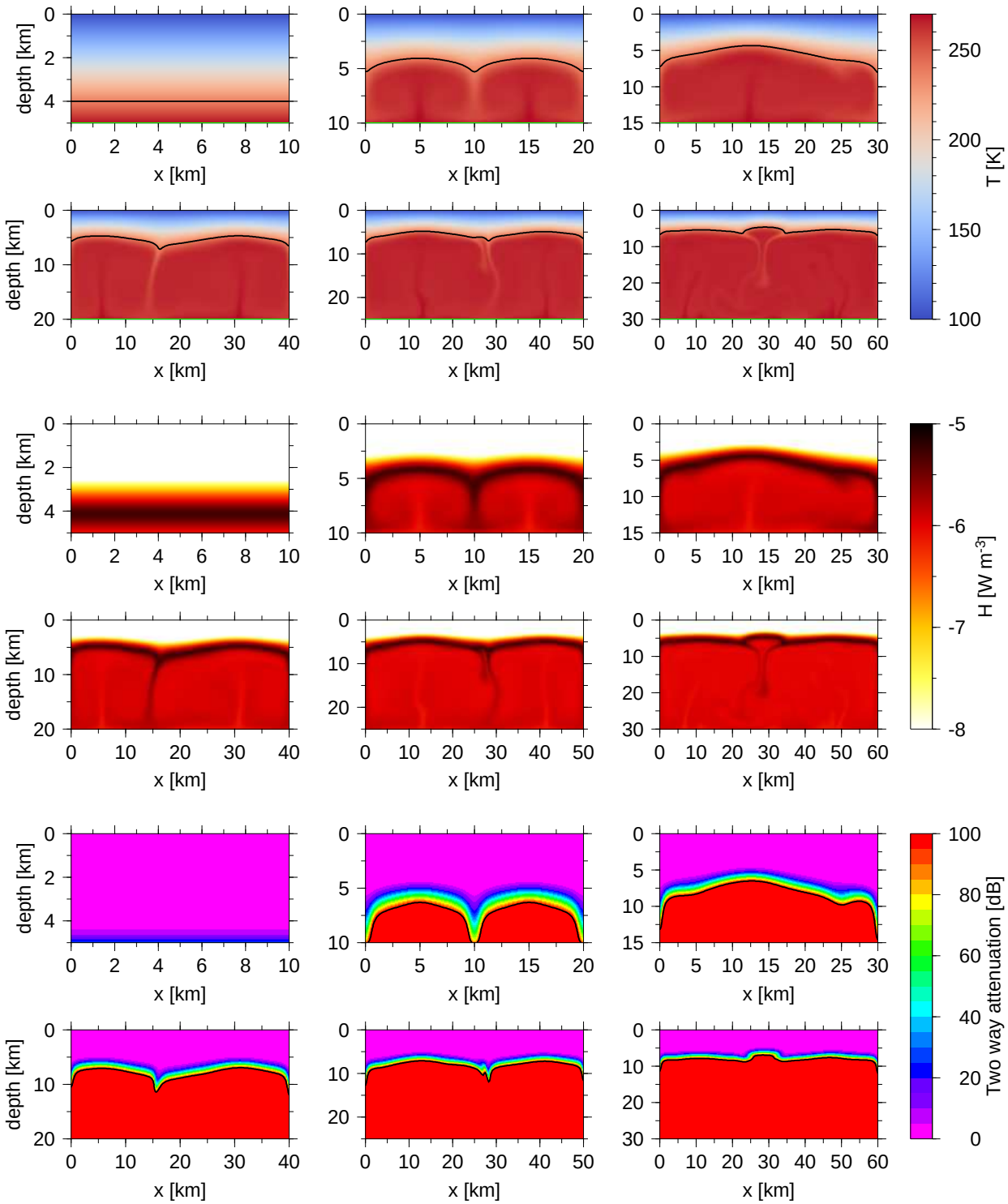

Figure S5: Results computed for: η_0=10^{13} Pa s, E_a=5×10^4 J mol^{-1}, T_s=100 K, H_m=5×10^{-6} W m^{-3}. Top: Temperature (black contour marks the eutectic temperature, T=237 K, green contour marks the melting temperature of 270 K), middle: heating rate, bottom: two-way attenuation for low loss ice (black contour marks the attenuation of 100 dB).

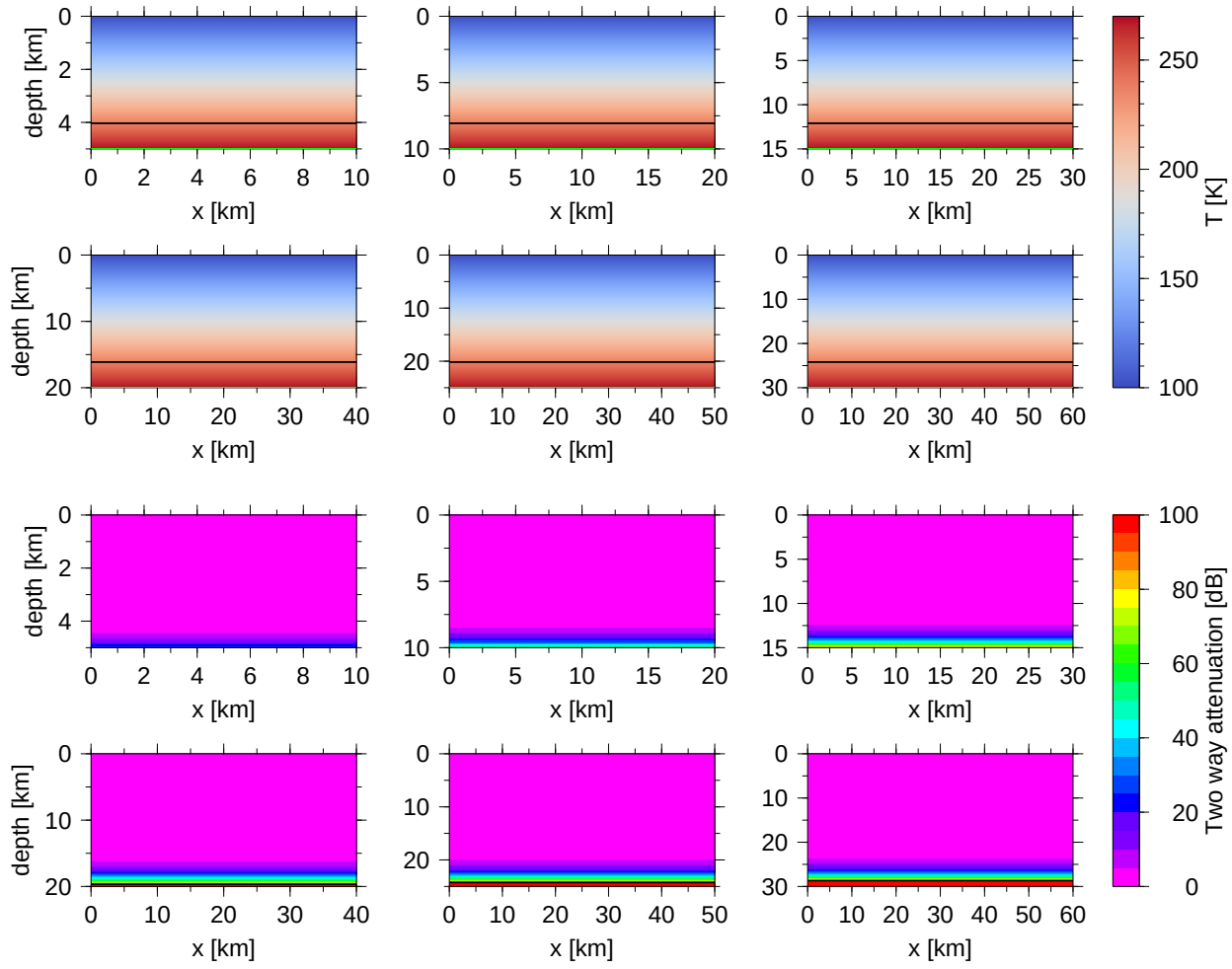

Figure S6: Results computed for: η_0=10^{15} Pa s, E_a=5×10^4 J mol^{-1}, T_s=100 K, H_m=0×10^{-6} W m^{-3}. Top: Temperature (black contour marks the eutectic temperature, T=237 K, green contour marks the melting temperature of 270 K), bottom: two-way attenuation for low loss ice (black contour marks the attenuation of 100 dB).

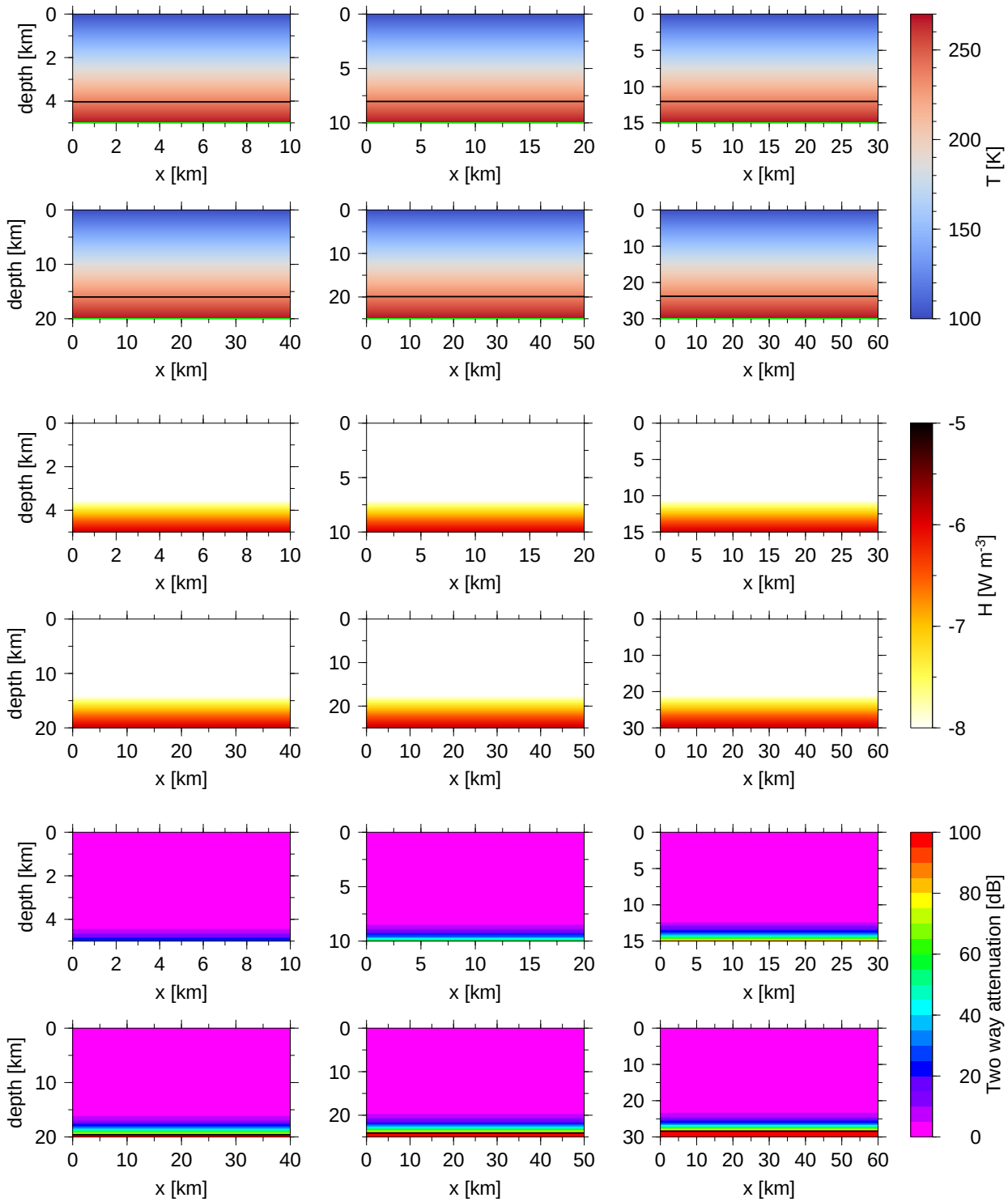

Figure S7: Results computed for: η_0=10^{15} Pa s, E_a=5×10^4 J mol^{-1}, T_s=100 K, H_m=5×10^{-6} W m^{-3}. Top: Temperature (black contour marks the eutectic temperature, T=237 K, green contour marks the melting temperature of 270 K), middle: heating rate, bottom: two-way attenuation for low loss ice (black contour marks the attenuation of 100 dB).

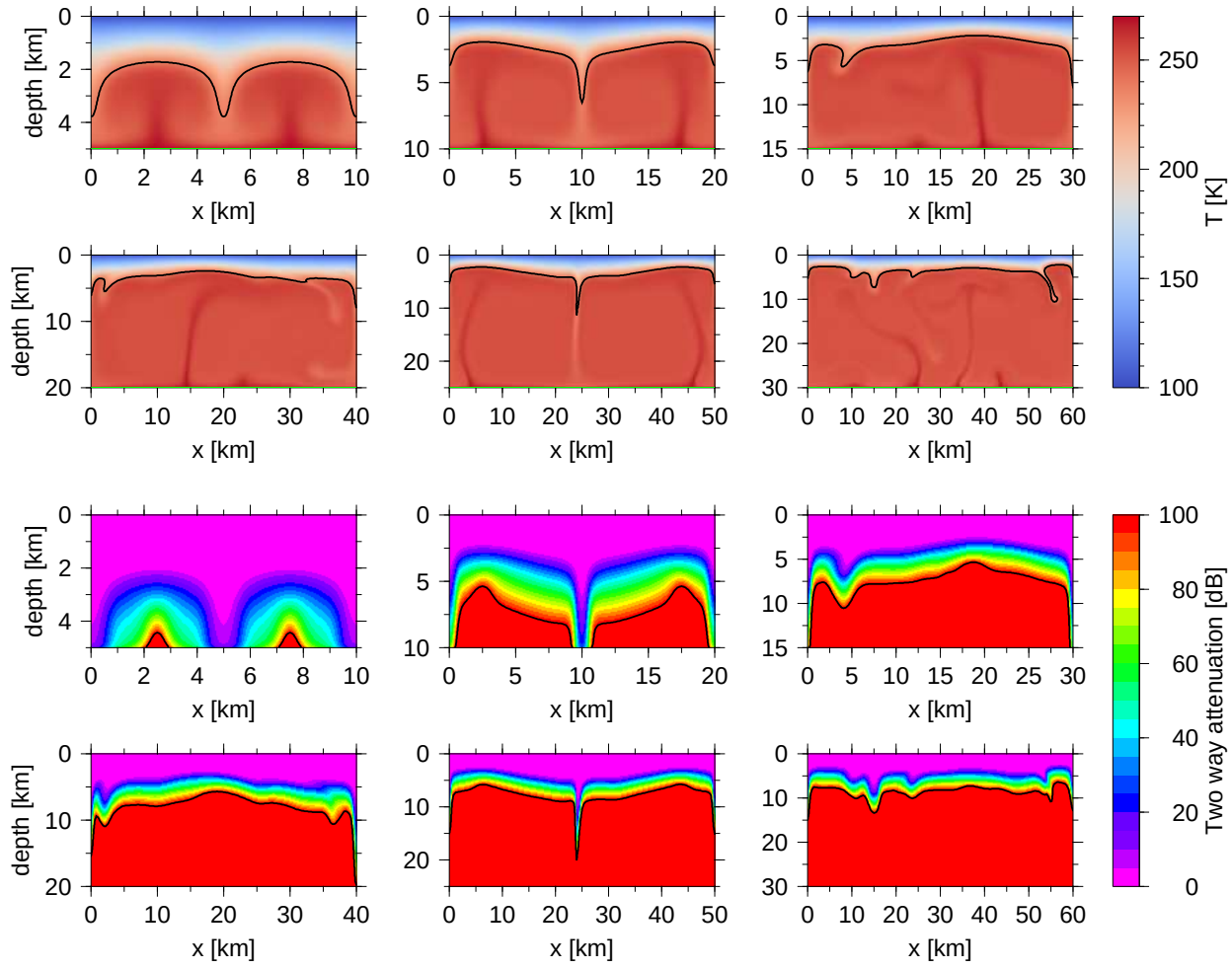

Figure S8: Results computed for: η_0=10^{13} Pa s, E_a=2.2×10^4 J mol^{-1}, T_s=100 K, H_m=0×10^{-6} W m^{-3}. Top: Temperature (black contour marks the eutectic temperature, T=237 K, green contour marks the melting temperature of 270 K), bottom: two-way attenuation for low loss ice (black contour marks the attenuation of 100 dB).

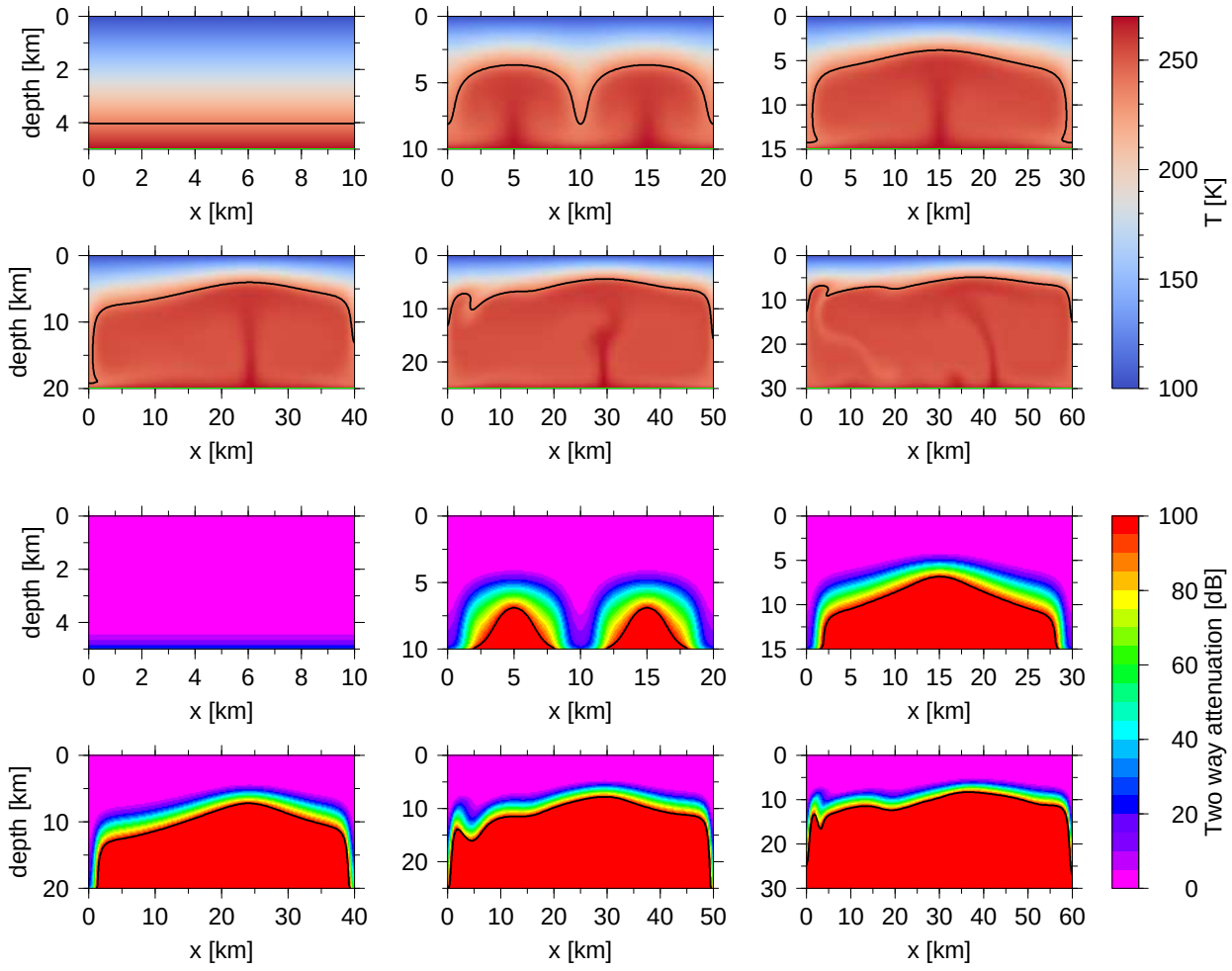

Figure S9: Results computed for: η_0=10^{14} Pa s, E_a=2.2×10^4 J mol^{-1}, T_s=100 K, H_m=0×10^{-6} W m^{-3}. Top: Temperature (black contour marks the eutectic temperature, T=237 K, green contour marks the melting temperature of 270 K), bottom: two-way attenuation for low loss ice (black contour marks the attenuation of 100 dB).

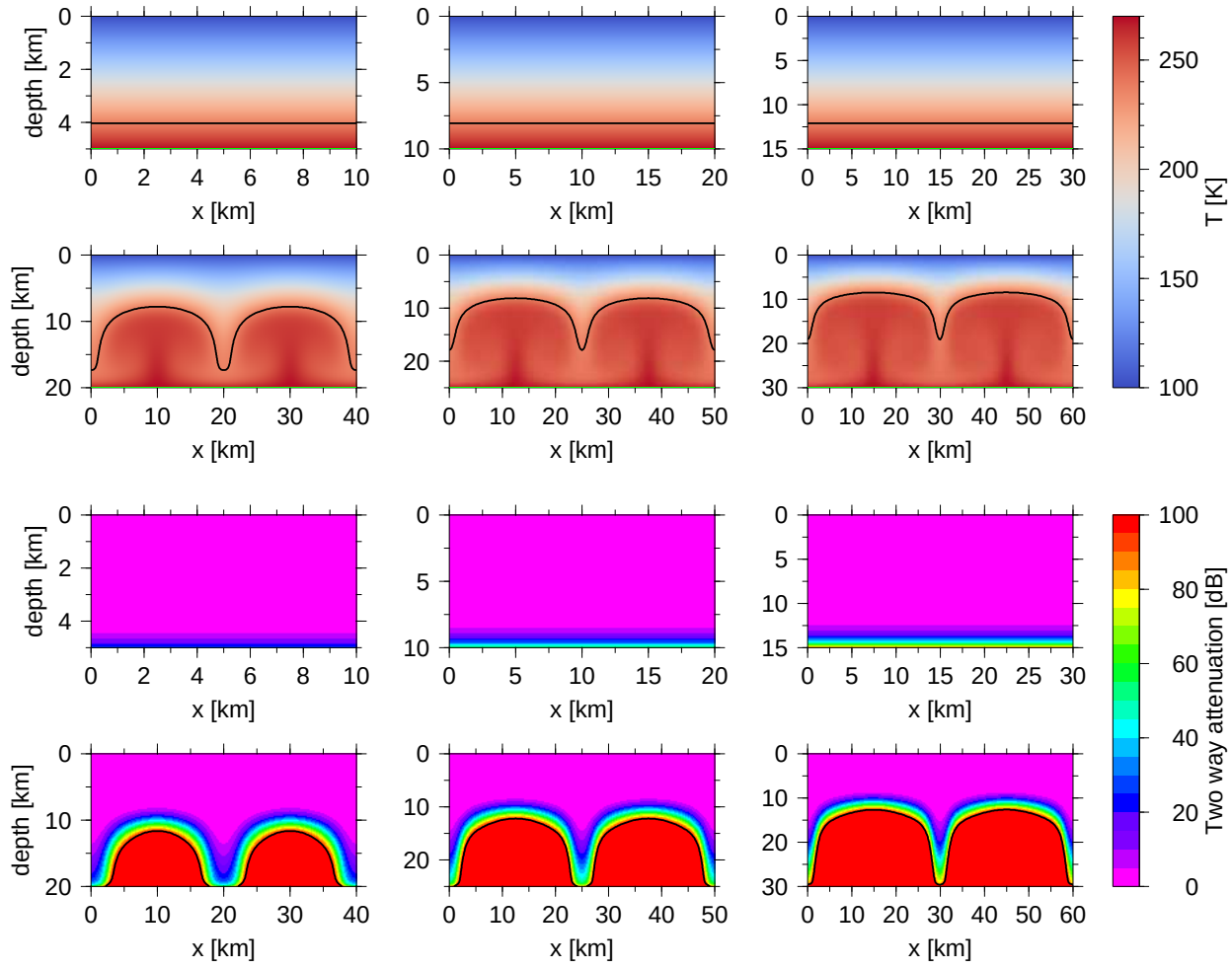

Figure S10: Results computed for: η_0=10^{15} Pa s, E_a=2.2×10^4 J mol^{-1}, T_s=100 K, H_m=0×10^{-6} W m^{-3}. Top: Temperature (black contour marks the eutectic temperature, T=237 K, green contour marks the melting temperature of 270 K), bottom: two-way attenuation for low loss ice (black contour marks the attenuation of 100 dB).

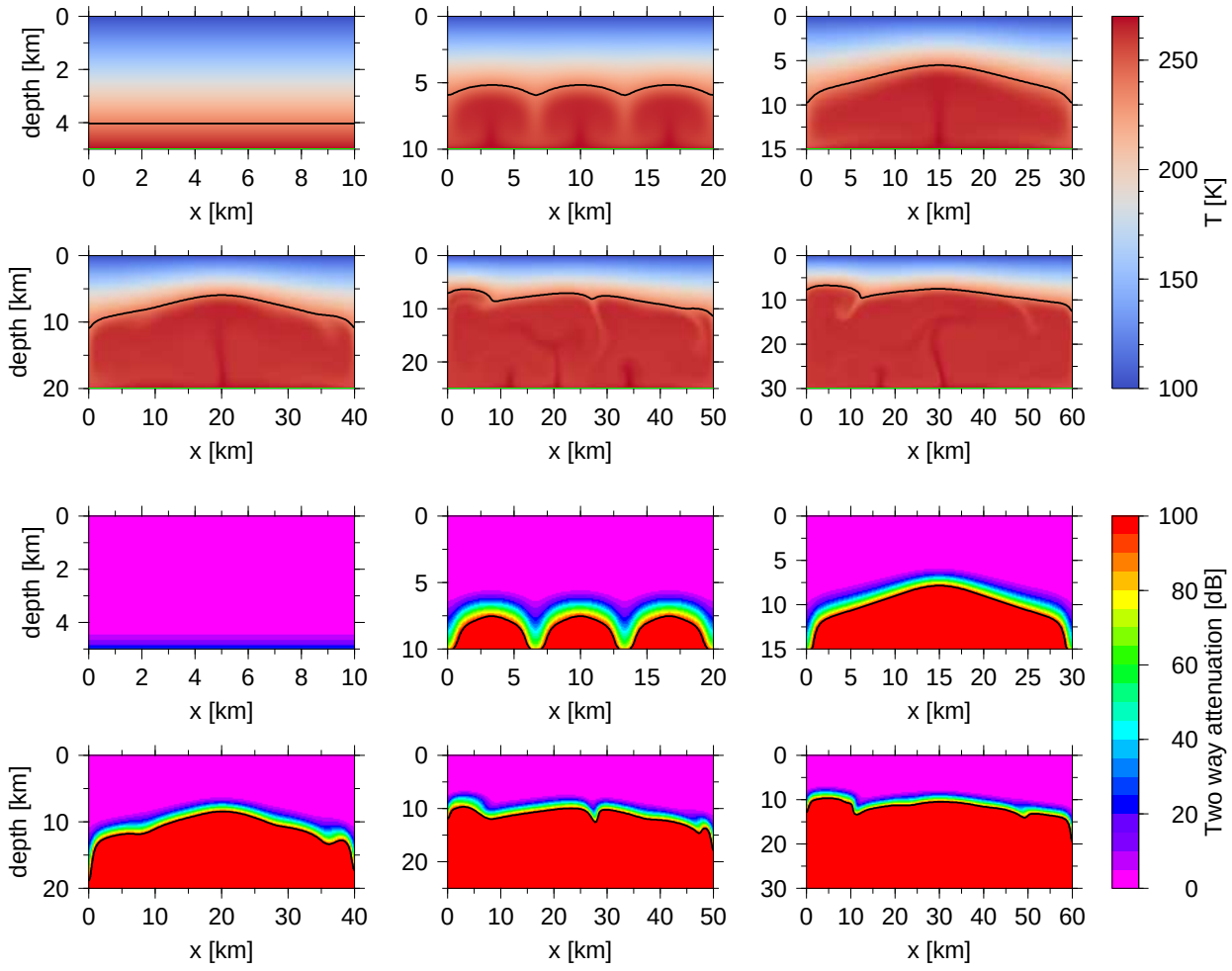

Figure S11: Results computed for: η_0=10^{13} Pa s, E_a=6×10^4 J mol^{-1}, T_s=100 K, H_m=0×10^{-6} W m^{-3}. Top: Temperature (black contour marks the eutectic temperature, T=237 K, green contour marks the melting temperature of 270 K), bottom: two-way attenuation for low loss ice (black contour marks the attenuation of 100 dB).

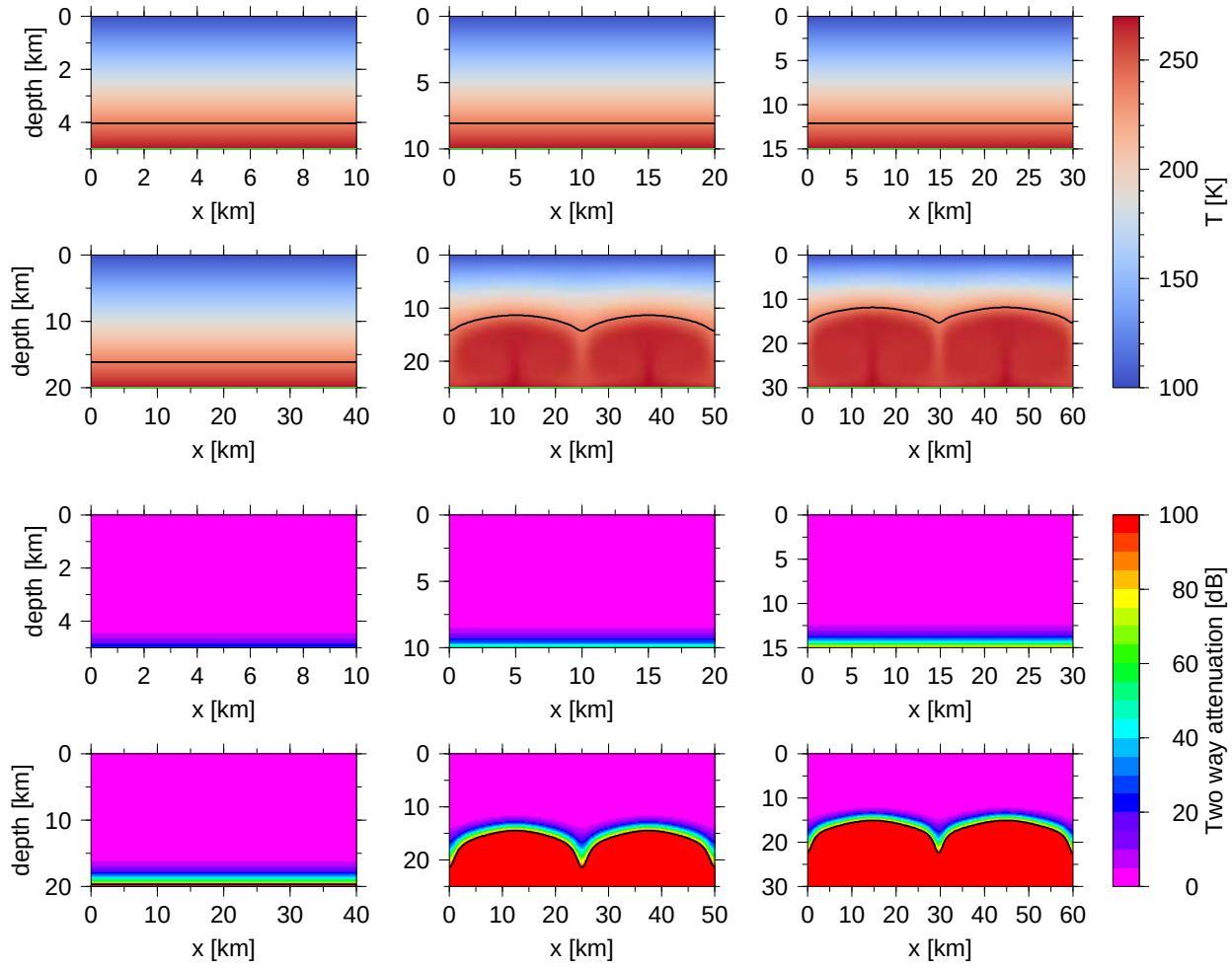

Figure S12: Results computed for: η_0=10^{14} Pa s, E_a=6×10^4 J mol^{-1}, T_s=100 K, H_m=0×10^{-6} W m^{-3}. Top: Temperature (black contour marks the eutectic temperature, T=237 K, green contour marks the melting temperature of 270 K), bottom: two-way attenuation for low loss ice (black contour marks the attenuation of 100 dB).

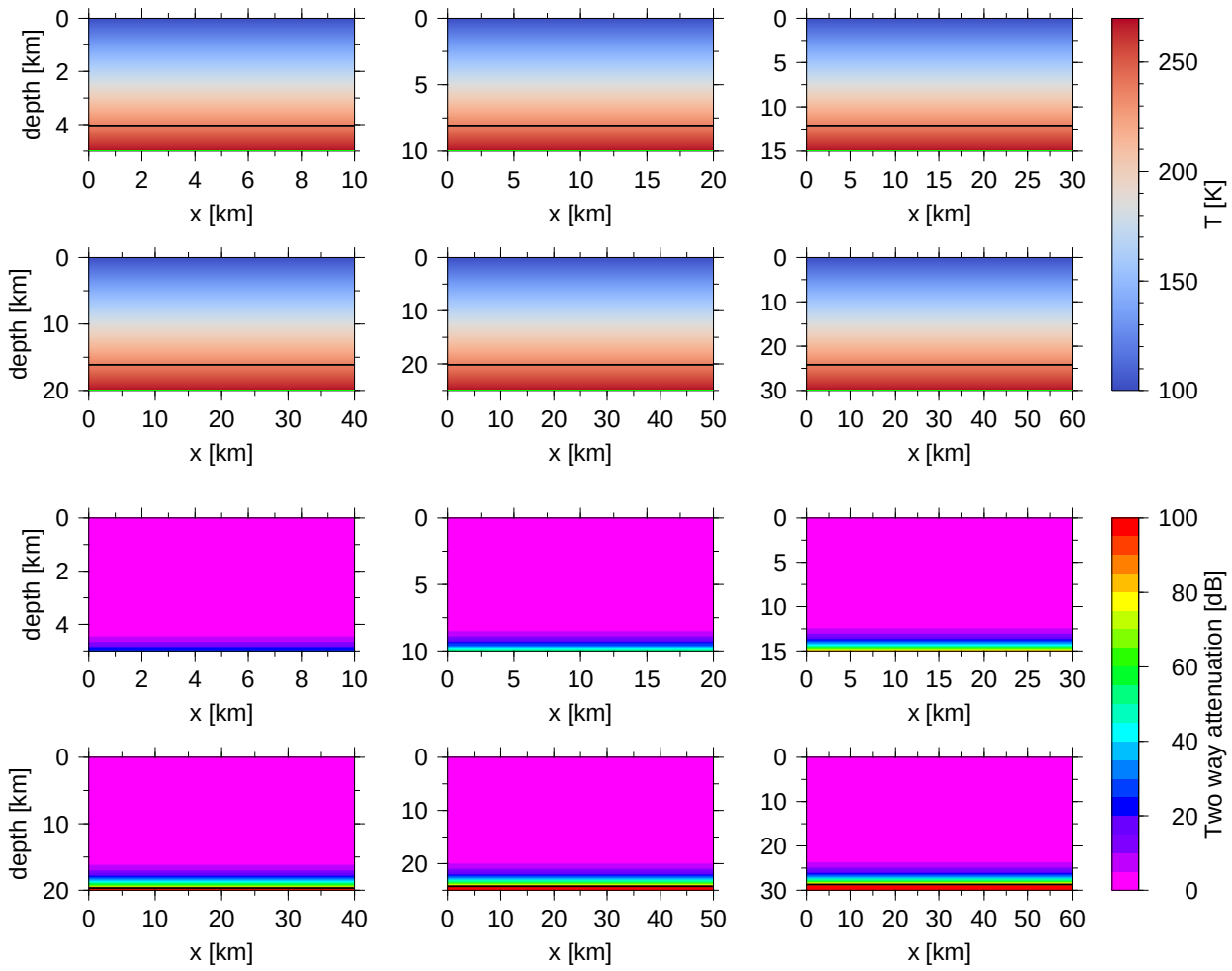

Figure S13: Results computed for: η_0=10^{15} Pa s, E_a=6×10^4 J mol^{-1}, T_s=100 K, H_m=0×10^{-6} W m^{-3}. Top: Temperature (black contour marks the eutectic temperature, T=237 K, green contour marks the melting temperature of 270 K), bottom: two-way attenuation for low loss ice (black contour marks the attenuation of 100 dB).

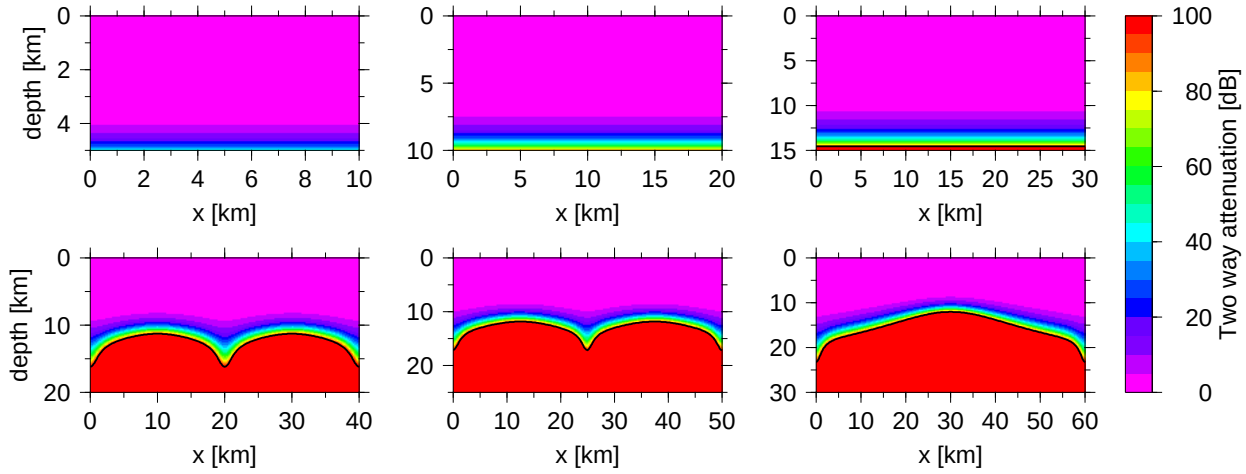

Figure S14: Results computed for: η_0=10^{14} Pa s, E_a=5×10^4 J mol^{-1}, T_s=100 K, H_m=0×10^{-6} W m^{-3}. Two-way attenuation for high loss ice (black contour marks the attenuation of 100 dB).

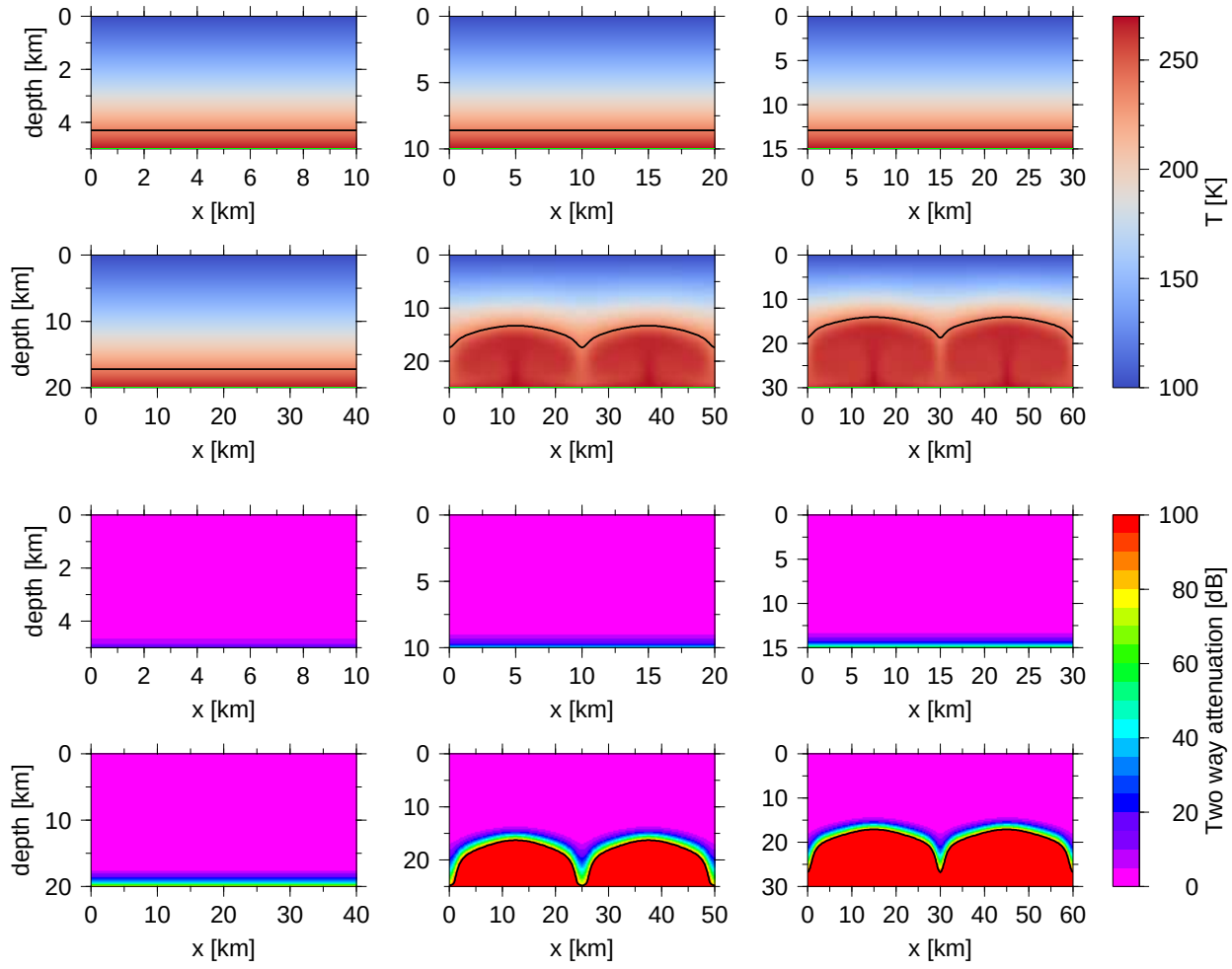

Figure S15: Results computed for: η_0=10^{14} Pa s, E_a=5×10^4 J mol^{-1}, T_s=100 K, H_m=0×10^{-6} W m^{-3}, k=$f(T)$. Top: Temperature (black contour marks the eutectic temperature, T=237 K, green contour marks the melting temperature of 270 K), bottom: two-way attenuation for low loss ice (black contour marks the attenuation of 100 dB).

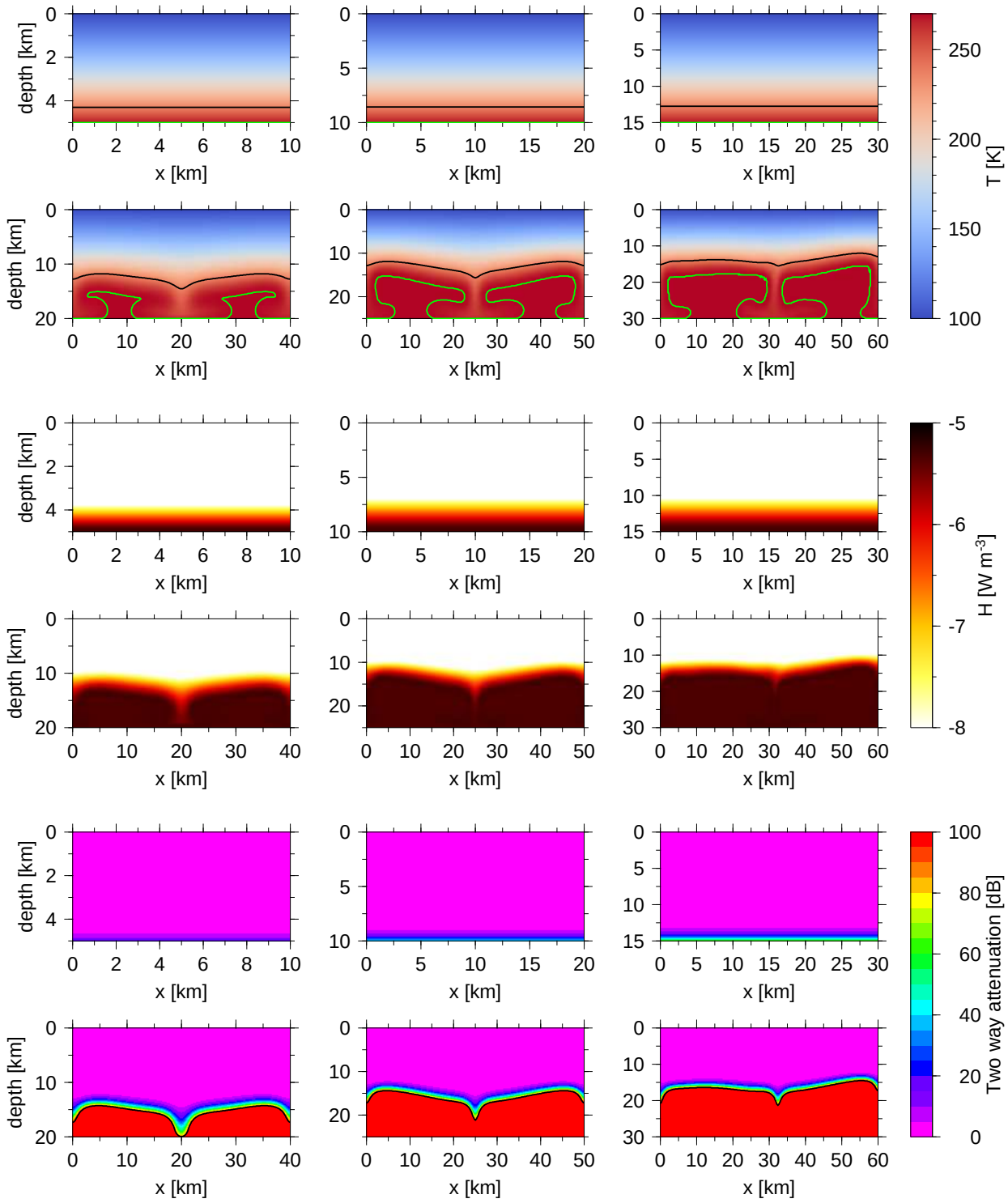

Figure S16: Results computed for: η_0=10^{14} Pa s, E_a=5×10^4 J mol^{-1}, T_s=100 K, H_m=5×10^{-6} W m^{-3}, k=$f(T)$. Top: Temperature (black contour marks the eutectic temperature, T=237 K, green contour marks the melting temperature of 270 K), middle: heating rate, bottom: two-way attenuation for low loss ice (black contour marks the attenuation of 100 dB).

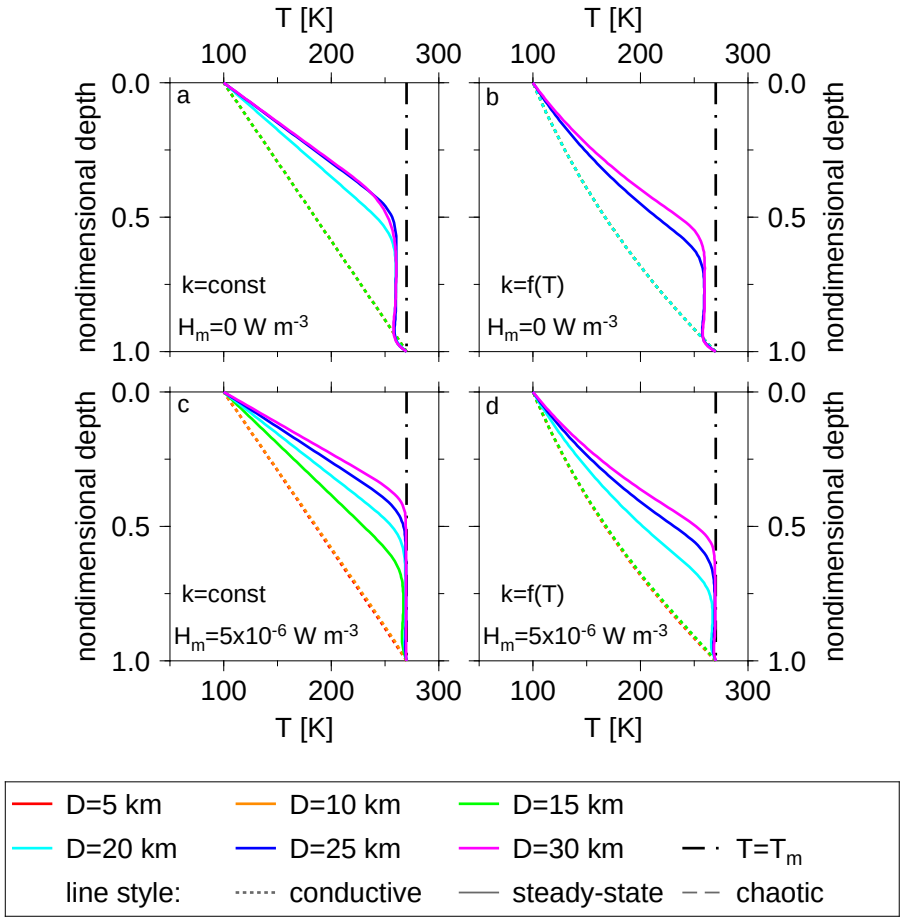

Figure S17: Horizontally-averaged temperature profiles (depth is nondimensionalized) for η_0=10^{14} Pa s, E_a=5×10^4 J mol^{-1}, T_s=100 K, H_m=0×10^{-6} W m^{-3} (top) or H_m=5×10^{-6} W m^{-3} (bottom), k=const. (left column) vs. k=$f(T)$ (right column). Colors represent the various shell thicknesses (5, 10, 15, 20, 25, and 30 km), line textures correspond to thermal states: conductive (dotted), convective steady-state (solid), convective chaotic (dashed). The vertical black dot-dashed line marks the melting temperature.

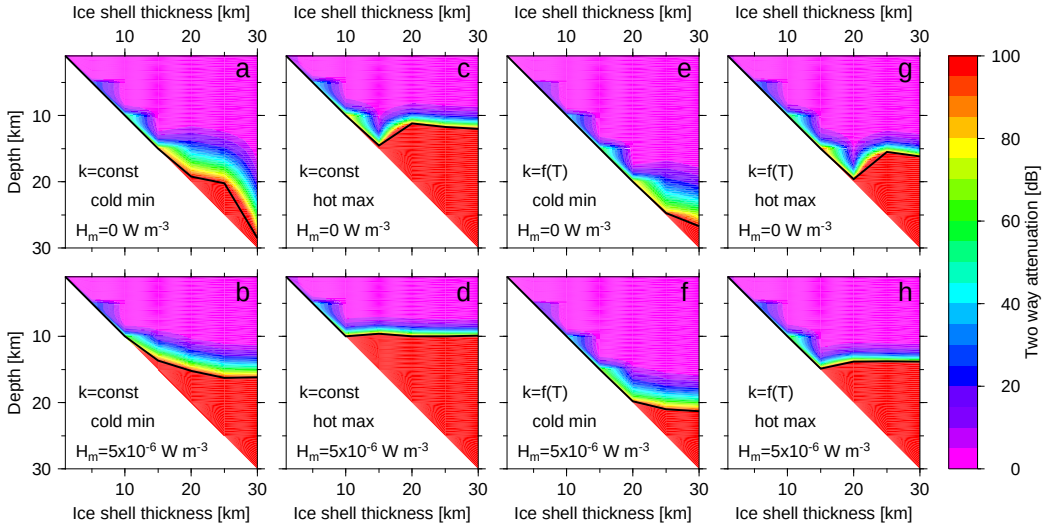

Figure S18: Two-way attenuation as a function of depth and shell thickness evaluated for η_0=10^{14} Pa s, E_a=5×10^4 J mol^{-1}, T_s=100 K, H_m=0×10^{-6} W m^{-3} (top) or H_m=5×10^{-6} W m^{-3} (bottom), low loss (first and third columns) vs high loss (second and fourth columns), k=const. (first and second columns) vs k=$f(T)$ (third and fourth columns). The solid black lines denote the penetration depth (considering the value of 100 dB as an upper limit).

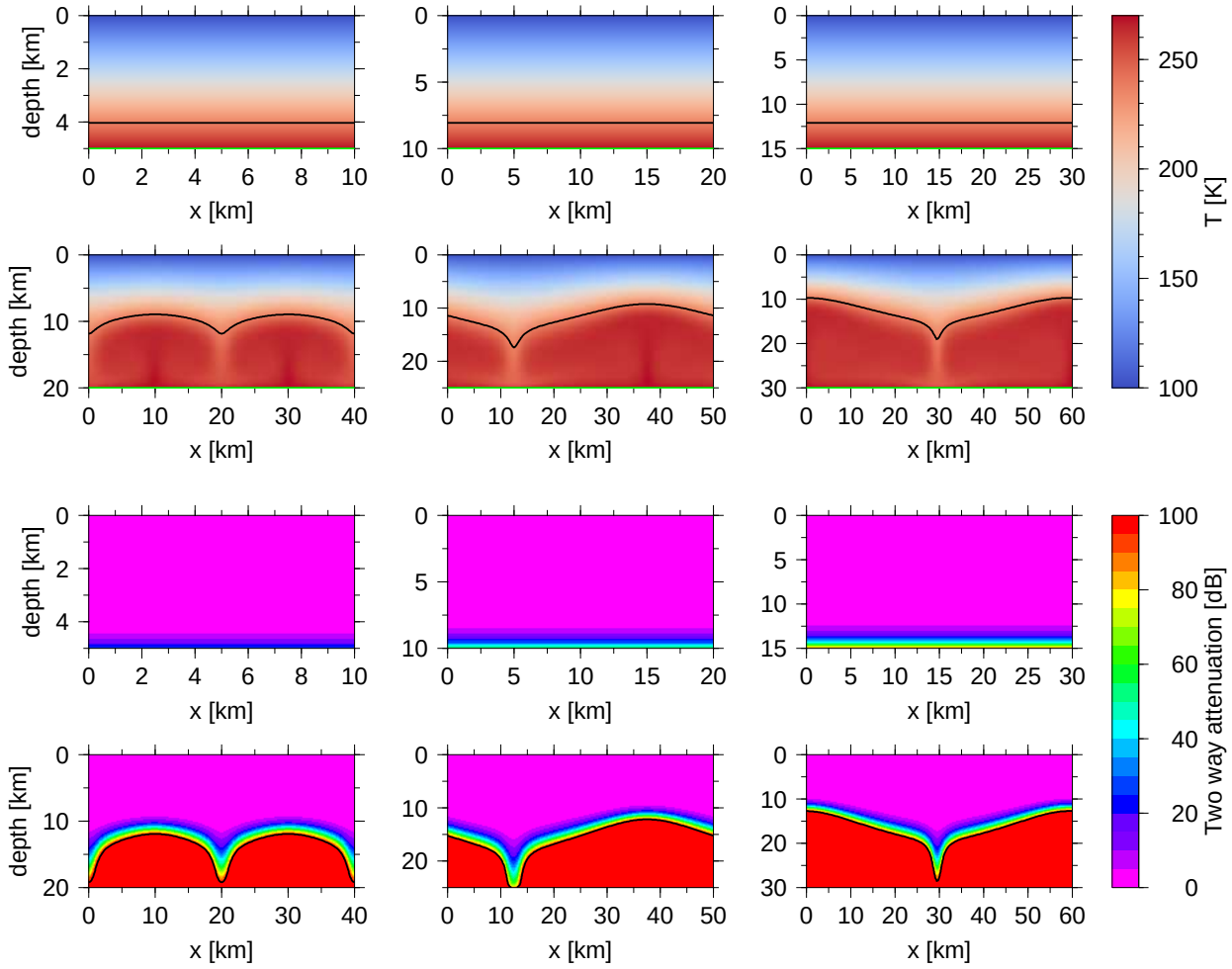

Figure S19: Results computed for: η_0=10^{14} Pa s, E_a=5×10^4 J mol^{-1}, T_s=100 K, H_m=0×10^{-6} W m^{-3}, and periodic boundary conditions. Top: Temperature (black contour marks the eutectic temperature, T=237 K, green contour marks the melting temperature of 270 K), bottom: two-way attenuation for low loss ice (black contour marks the attenuation of 100 dB).

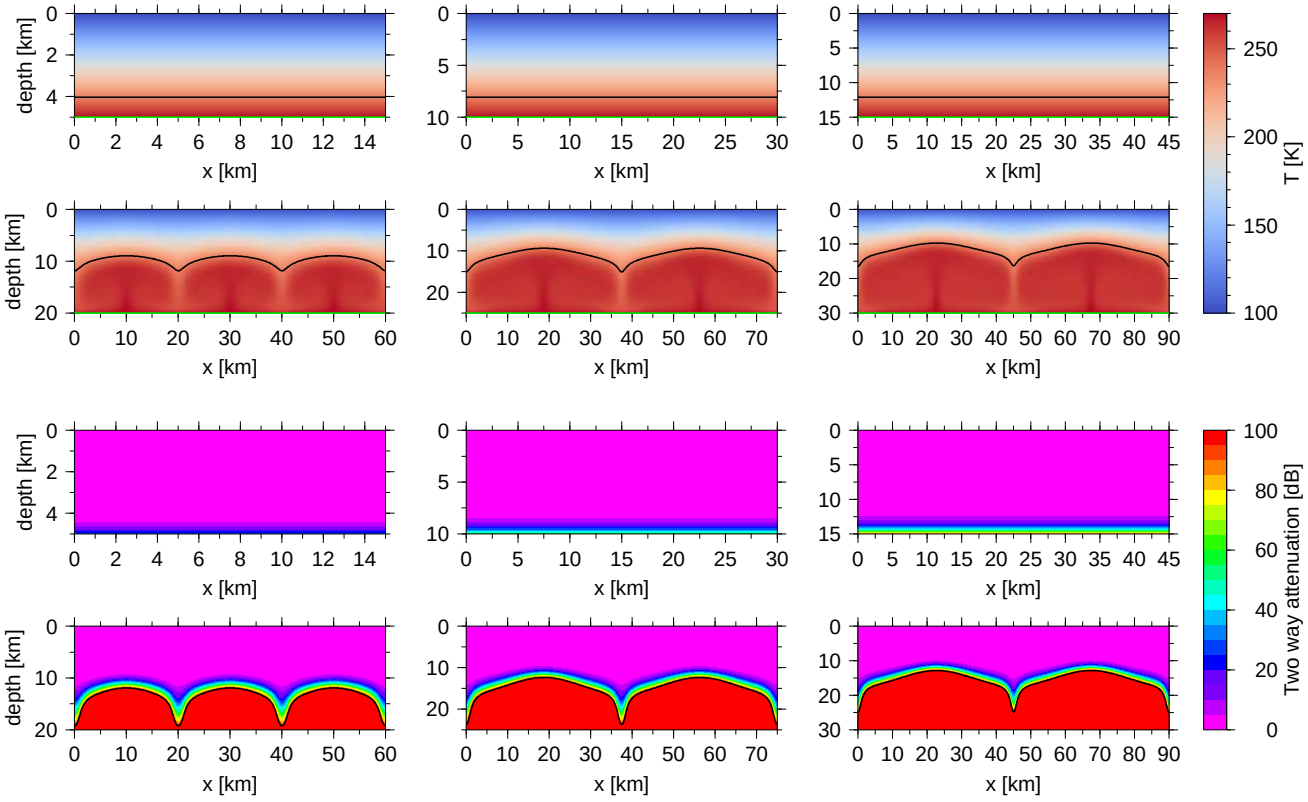

Figure S20: Results computed for: η_0=10^{14} Pa s, E_a=5×10^4 J mol^{-1}, T_s=100 K, H_m=0×10^{-6} W m^{-3}, and aspect ratio λ=3. Top: Temperature (black contour marks the eutectic temperature, T=237 K, green contour marks the melting temperature of 270 K), bottom: two-way attenuation for low loss ice (black contour marks the attenuation of 100 dB).

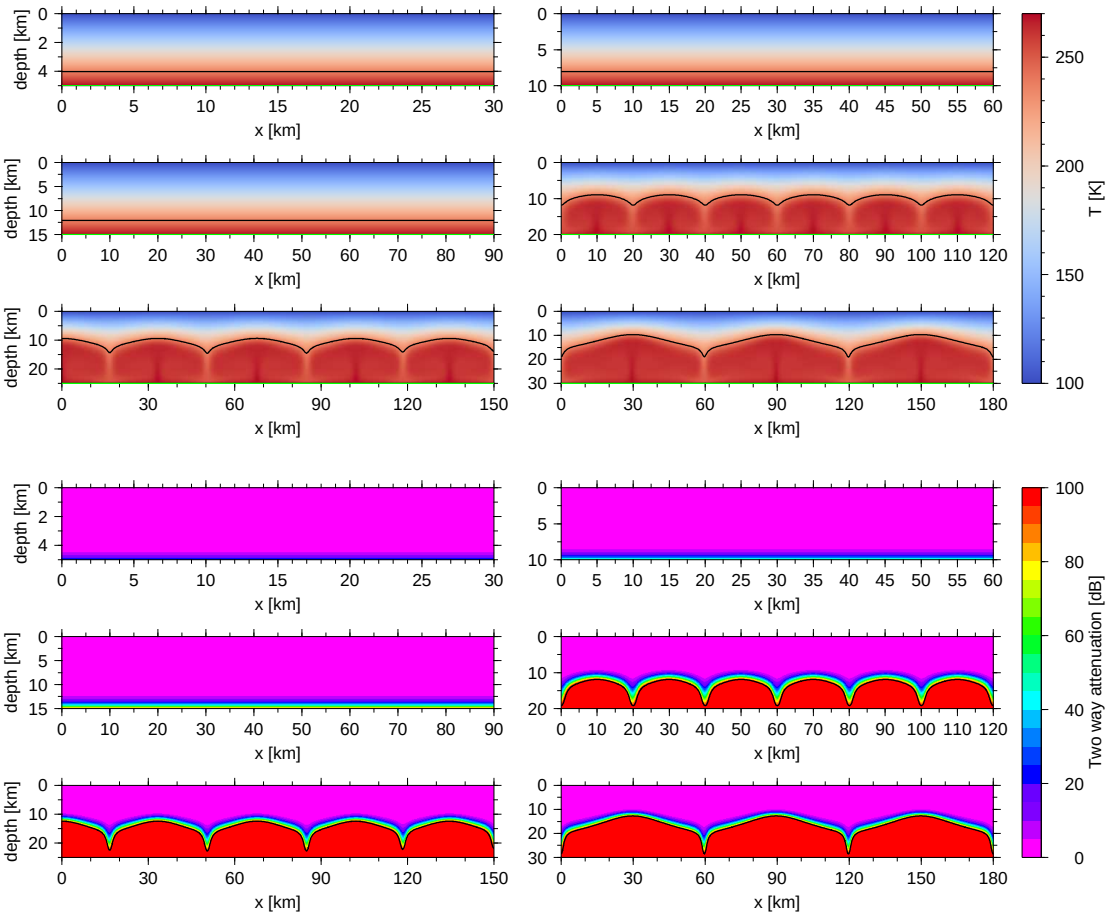

Figure S21: Results computed for: η_0=10^{14} Pa s, E_a=5×10^4 J mol^{-1}, T_s=100 K, H_m=0×10^{-6} W m^{-3}, and aspect ratio λ=6. Top: Temperature (black contour marks the eutectic temperature, T=237 K, green contour marks the melting temperature of 270 K), bottom: two-way attenuation for low loss ice (black contour marks the attenuation of 100 dB).

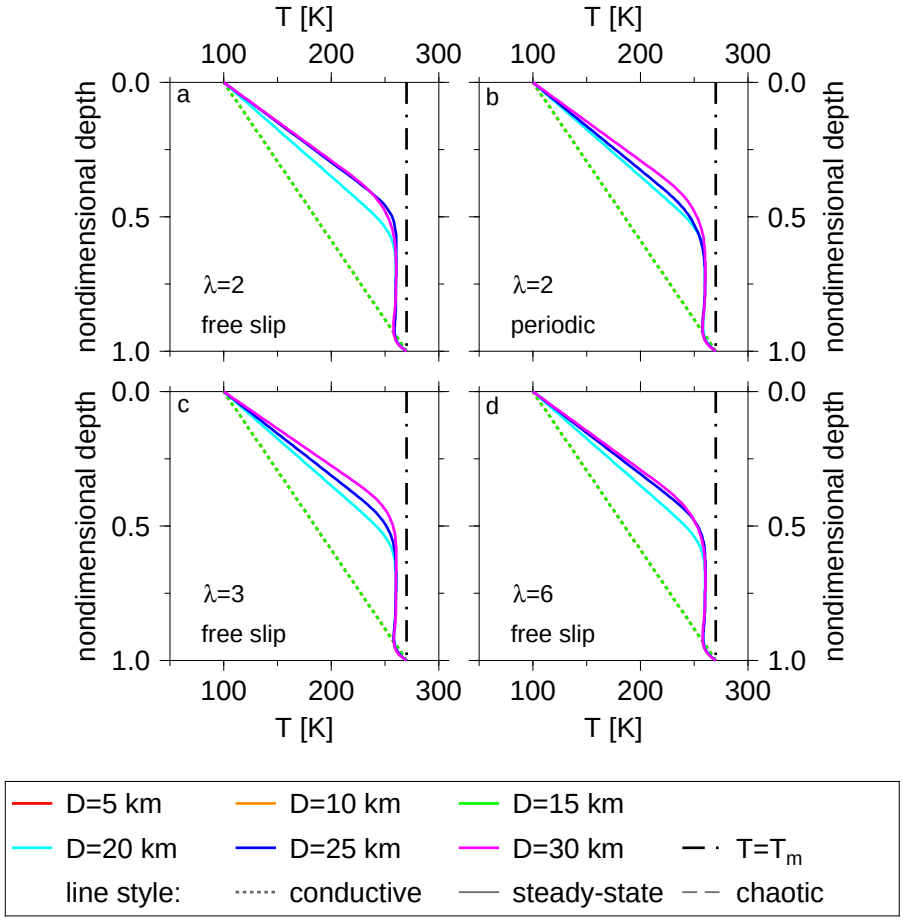

Figure S22: Horizontally-averaged temperature profiles (depth is nondimensionalized) for η_0=10^{14} Pa s, E_a=5×10^4 J mol^{-1}, T_s=100 K, and H_m=0×10^{-6} W m^{-3}. Reference simulation (free slip, λ=2, top left), simulation R1 (periodic boundary condition, λ=2, top right), simulation R2 (free slip, λ=3, botom left), and simulation R3 (free slip, λ=6, botom right). Colors represent the various shell thicknesses (5, 10, 15, 20, 25, and 30 km), line textures correspond to thermal states: conductive (dotted), convective steady-state (solid), convective chaotic (dashed). The vertical black dot-dashed line marks the melting temperature.

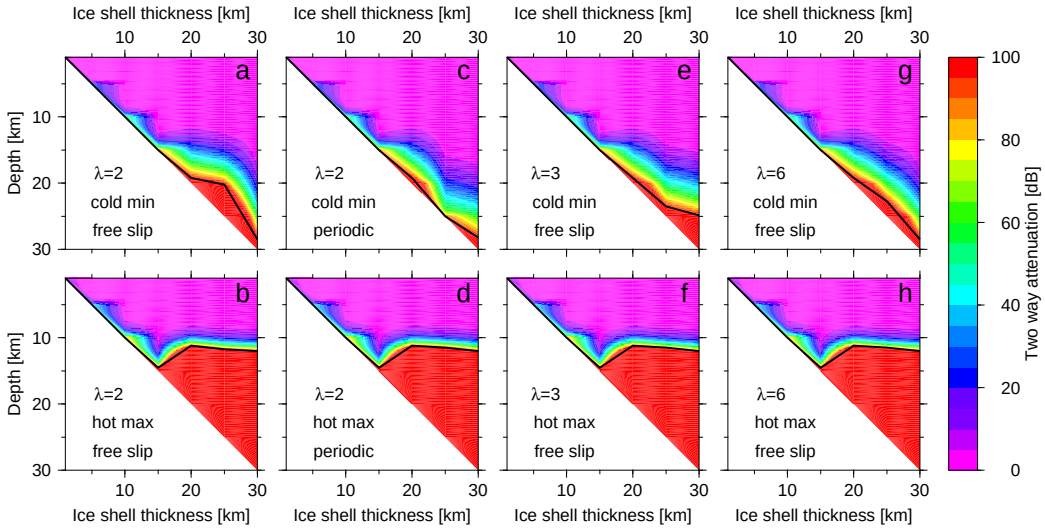

Figure S23: Two-way attenuation as a function of depth and shell thickness evaluated for η_0=10^{14} Pa s, E_a=5×10^4 J mol^{-1}, T_s=100 K, and H_m=0×10^{-6} W m^{-3}. Reference simulation: panels a (cold downwelling & low loss ice) and b (hot upwelling & high loss ice), simulation R1: panels c and d, simulation R2: panels e and f, and simulation R3: panels g and h. The solid black lines denote the penetration depth (considering the value of 100 dB as an upper limit).

Table S1: Thermal regimes together with maximum (cold downwelling & low loss ice, left number in each cell) and minimum (hot upwelling & high loss ice, right number in each cell) penetration depths for η_0=10^{14} Pa s, E_a=5×10^4 J mol^{-1}, T_s=100 K, two volumetric heating amplitudes H_m=0 W m^{-3} and H_m=5×10^{-6} W m^{-3} and various shell thicknesses D. Comparison of results computed for constant and temperature-dependent thermal conductivity, respectively. The cell color corresponds to the relative penetration depth: **ocean is reached**, **≥75% of the shell thickness is penetrated**, **50–75% of the shell thickness is penetrated**, **<50% of the shell thickness is penetrated**. The transition between thermal regimes (conductive / convective steady-state / convective chaotic) is marked by thick lines with conductive regimes at bottom left and convective chaotic regimes at top right.

D	5 km		10 km		15 km		20 km		25 km		30 km	
E_a=5×10^4 J mol^{-1}, η_0=10^{14} Pa s, T_s=100 K, H_m=0 W m^{-3}												
k=const.	**5.0**	**5.0**	**10.0**	**10.0**	**15.0**	**14.6**	**19.2**	**11.2**	**20.2**	**11.8**	**28.5**	**12.0**
k=$f(T)$	**5.0**	**5.0**	**10.0**	**10.0**	**15.0**	**15.0**	**20.0**	**19.6**	**24.8**	**15.5**	**26.7**	**16.2**
E_a=5×10^4 J mol^{-1}, η_0=10^{14} Pa s, T_s=100 K, H_m=5×10^{-6} W m^{-3}												
k=const.	**5.0**	**5.0**	**10.0**	**10.0**	**13.7**	**9.6**	**15.2**	**10.0**	**16.3**	**10.0**	**16.2**	**9.9**
k=$f(T)$	**5.0**	**5.0**	**10.0**	**10.0**	**15.0**	**14.9**	**19.8**	**13.8**	**21.0**	**13.8**	**21.3**	**13.8**

Table S2: Thermal regimes together with maximum (cold downwelling & low loss ice, left number in each cell) and minimum (hot upwelling & high loss ice, right number in each cell) penetration depths for η_0=10^{14} Pa s, E_a=5×10^4 J mol^{-1}, T_s=100 K, H_m=0 W m^{-3} and various shell thicknesses D. Comparison of reference simulation with the simulations R1–R3 (cf. text). The cell color corresponds to the relative penetration depth: **ocean is reached**, **≥75% of the shell thickness is penetrated**, **50–75% of the shell thickness is penetrated**, **<50% of the shell thickness is penetrated**. The transition between thermal regimes (conductive / convective steady-state / convective chaotic) is marked by thick lines with conductive regimes at bottom left and convective chaotic regimes at top right.

D	5 km		10 km		15 km		20 km		25 km		30 km	
E_a=5×10^4 J mol^{-1}, η_0=10^{14} Pa s, T_s=100 K, H_m=0 W m^{-3}												
λ=2, free slip	**5.0**	**5.0**	**10.0**	**10.0**	**15.0**	**14.6**	**19.2**	**11.2**	**20.2**	**11.8**	**28.5**	**12.0**
λ=2, periodic	**5.0**	**5.0**	**10.0**	**10.0**	**15.0**	**14.6**	**19.2**	**11.2**	**25.0**	**11.5**	**28.2**	**12.0**
λ=3, free slip	**5.0**	**5.0**	**10.0**	**10.0**	**15.0**	**14.6**	**19.2**	**11.2**	**23.5**	**11.5**	**24.9**	**12.0**
λ=6, free slip	**5.0**	**5.0**	**10.0**	**10.0**	**15.0**	**14.6**	**19.2**	**11.2**	**22.8**	**11.5**	**28.5**	**12.0**